A Single-Nucleotide Polymorphism of Human Neuropeptide S Gene Originated from Europe Shows Decreased Bioactivity

Cheng Deng[1]*[9], Ximiao He[2][9], Aaron J. W. Hsueh[1]*

1 Program of Reproductive and Stem Cell Biology, Department of Ob/Gyn, Stanford University School of Medicine, Stanford, California, United States of America, **2** National Cancer Institute, National Institutes of Health, Bethesda, Maryland, United States of America

Abstract

Using accumulating SNP (Single-Nucleotide Polymorphism) data, we performed a genome-wide search for polypeptide hormone ligands showing changes in the mature regions to elucidate genotype/phenotype diversity among various human populations. Neuropeptide S (NPS), a brain peptide hormone highly conserved in vertebrates, has diverse physiological effects on anxiety, fear, hyperactivity, food intake, and sleeping time through its cognate receptor-NPSR. Here, we report a SNP *rs4751440* (L^6-NPS) causing non-synonymous substitution on the 6th position (V to L) of the NPS mature peptide region. L^6-NPS has a higher allele frequency in Europeans than other populations and probably originated from European ancestors ~25,000 yrs ago based on haplotype analysis and Approximate Bayesian Computation. Functional analyses indicate that L^6-NPS exhibits a significant lower bioactivity than the wild type NPS, with ~20-fold higher EC_{50} values in the stimulation of NPSR. Additional evolutionary and mutagenesis studies further demonstrate the importance of the valine residue in the 6th position for NPS functions. Given the known physiological roles of NPS receptor in inflammatory bowel diseases, asthma pathogenesis, macrophage immune responses, and brain functions, our study provides the basis to elucidate NPS evolution and signaling diversity among human populations.

Introduction

In two randomly selected human genomes, 99.9% of the DNA sequence is identical and the remaining 0.1% accounts for variations among individuals [1–3]. SNP (Single-Nucleotide Polymorphism) is the simplest form of genetic variations, occurring at a frequency of about 1 per 1,000 bp in human chromosomes [4]. Identifying important SNPs which underlie regional adaptations is a key to understanding genetic diversities among different human populations. More and more adaptive traits resulting from one single SNP have been elucidated in selective human populations. For polypeptide ligands and receptors, a GIP (gastric inhibitory polypeptide) SNP with altered bioactivity was shown to be the result of adaptive selection in Eurasian populations [5] whereas an SNP of the EDAR gene was found to increase the number of active eccrine glands in the Han Chinese [6]. In addition, a Leu7Pro polymorphism in the signal peptide region of the NPY (neuropeptide Y) gene has been found to show higher plasma NPY levels in response to physiological stress and is associated with a greater risk of developing alcohol dependence in patients [7]. Also, two SNPs found in the chemokine receptor CX3CR1 gene of Caucasians were shown to be more responsive to the chemokine ligand fractalkine and confer rapid progression to AIDS [8]. With the completion of more SNP projects, we can better elucidate the genetic diversity of polypeptide ligands among different human populations during evolution.

Neuropeptide S (NPS) is a conserved 20-amino-acid peptide found in mammals and identified as a neuromodulator expressed in the brainstem [9]. *In vitro* studies demonstrated that NPS binds specifically to NPSR, a G protein-coupled receptor, to increase cAMP production and intracellular Ca^{2+} levels [9,10]. NPS and its receptor-NPSR are expressed in various tissues in rodents, with the highest levels in brain, thyroid, salivary, and mammary glands [9]. In the brainstem, the NPS highly expressed in three groups of neurons located between the locus coeruleus (LC) and Barrington's nucleus. The first and second groups of NPS-expressing neurons co-expressed with the glutamatergic neurons and are localized to the locus coeruleus and principle sensory nucleus, respectively. In contrast, the third NPS-expressing neuron group is localized to the lateral parabrachial nucleus and later is indentified to co-express the corticotropin-releasing factor (CRF) [9,11–14]. In contrast to NPS, its receptor NPSR shows a wider expression pattern in the brain. The highest expression of NPSR was found in areas involved in olfactory function, including the anterior olfactory nucleus, the endopiriform nucleus, and the piriform cortex [11–13]. NPSR is also expressed in several brain regions mediating anxiety responses, including the amygdaloid complex and the paraventricular hypothalamic nucleus [11–13]. Also, NPSR is expressed in regions involved in sleep neurocircuitries,

such as the thalamus, the hypothalamus, and the preoptic region, as well as in the output and input regions of hippocampus, including the parahippocampal regions, the lateral entorhinal cortex, and the retrosplenial agranular cortex [11–13].

The wide expression pattern of NPSR implies that the NPS/NPSR system may be important for diverse brain functions. *In vivo* studies in mice showed that treatment with NPS suppresses anxiety and appetite [9,15,16], induces wakefulness and hyperactivity [17], decreases conditioned fear responses [12], stimulates the hypothalamic-pituitary-adrenal axis [18], and inhibits food intake [18].

Here, we found that a SNP *rs4751440* causing non-synonymous substitution at the 6th position (V to L) of the NPS mature peptide region has a relatively higher allele frequency in Europeans. This SNP variant (L6-NPS) shows a decreased ability to activate the NPSR receptor.

Materials and Methods

Haplotype Analysis

SNPs data from 1,092 samples were downloaded from the 1,000 Genome Project. After excluding monomorphic SNPs and SNPs with inconsistent genotypes, we obtained a final data set of 888 SNPs in 1,092 samples (2,184 chromosomes) from 14 populations. We inferred haplotype data by phasing with fastPHASE [19]. Examination of linkage disequilibrium patterns in the flanking regions revealed a ~14 kb block surrounding *rs4751440*. We counted the number of chromosomes for each haplotype in individual populations and plotted the haplotype frequencies on a world map.

Approximate Bayesian Computation

We used the spatially explicit population model [20] by considering evolutional process such as population structure, drift, and natural selection, as well as various demographic processes including population growth, sporadic long-range migration, and the effects of the spread of farming on carrying capacities, to implement the forward simulation. We applied an Approximate Bayesian Computation (ABC) inference framework to estimate parameters of interest [6,21]. Briefly, we employed spatially explicit forward simulations to model the origin and the subsequent spread of the derived *rs4751440* in Europe. The demic grid of this simulation model encompasses the geographic region between $35°N$ to $70°N$, and $20°W$ to $60°E$, covering all the available sampled populations in Europe. This geographic region was modeled as a series of 2,800 rectangular demes with each being one degree in latitude and one degree in longitude, which includes 1,573 land demes and 1,227 sea demes. The maximum population size in each deme (K_{deme}) is calculated as described by Itan et al. (2009) [22]: $K_{deme}=(0.2cl+0.8el)*D_{max}*A_{deme}$, where the cl is relative climate, with values of 0.25, 0.5, 0.75 and 1 for polar, cold, dry, and temperate climates respectively; the el is relative elevation; the A_{deme} is the area of the deme (km^2), and the D_{max} is the maximum population density which fixed as 5 individuals per km^2. Our simulations start from 40,000 yrs BP (1,600 generations ago, assuming 25 yrs per generation), because modern humans originated ~195,000 yrs ago in Sub-Saharan Africa and migrated towards Northern Eurasia ~40,000 yrs ago [23,24]. We assume the appearance of farmer as early as 7,000 yrs BP, and the allele of *rs4751440* appeared no later than 5,000 yrs BP. The population movements within and between demes, population growth and selection coefficient were simulated as described by Kamberov et al. (2013) [6]. At the end of each simulation, we recorded the parmeter values that generated the simulation, including the

genereation and the location (which deme) where the allele originated, and the derived allele frequency in 5 locations where observed allele frequency data available. We compared summary statistics (allele frequency of *rs4751440* in 5 populations) recorded after each simulation to observed frequencies, and accepted only those simulations with sufficiently small differences. We calculated the Euclidean distance (δ) between the simulated and observed statistics for each simulated data set and maintained those simulations with the smallest values. Among the total 3,000,000 simulations performed, we present parameter estimates using the best 0.03% (top 1,000) of the simulations, as well as we chose to base our inferences on the best 0.17% (top 5,000) in order to avoid over-fitting.

Materials

Full length cDNA for the NPSR receptor was purchased from OriGene Technologies. Different peptide variants (NPS, L6-NPS, A6-NPS, I6-NPS, F6-NPS, N6-NPS, K6-NPS, D6-NPS) were chemically synthesized by the Pan Facility at the Stanford University. In addition, wild type NPS and L6-NPS were chemically synthesized by NEO Group Inc. CRE- and NFAT luciferase reporter plasmids as well as the pSV-β-galactosidase control vectors were purchased from Promega.

Luciferase Assays

HEK293T cells seeded in 24-well plates were co-transfected with different luciferase reporters (50 ng), the pSV-β-Gal plasmid (5 ng), and the NPSR receptor plasmid (50 ng). After 36 h, cells were cultured in serum-free media for another 18 h with increasing doses of the various NPS peptides. Luciferase activities were determined using the luciferase assay kit (Promega) and normalized using β-galactosidase activities. All experiments were performed at least three times in triplicates. Data (EC_{50}) were analyzed using Graphpad Prism 5.0.

Results

Based on the new SNP database of the NHLBI GO Exome Sequencing Project (ESP), we screened the human genome for SNPs in the mature regions of all polypeptide ligands deposited in the Human Plasma Membrane receptome Database (HPMR; http://receptome.stanford.edu/HPMR/) [25,26]. As shown in Table S1, 339 SNPs and 59 SNPs were found to cause non-synonymous substitution in the mature regions in type A and B polypeptide ligands, respectively. Among different SNPs, we focused on the genotypic and allelic frequencies of the SNP *rs4751440*, locating on chromosome 10:129350856. This SNP was identified in both NHLBI GO Exome Sequencing Project (ESP) and International HapMap Project (Table 1 and 2). This SNP (G to C) causes non-synonymous amino acid substitution (V to L) in the NPS coding region. Both databases showed higher allele frequencies (about 13%) for L6-NPS in Europeans than other populations, with about 22% heterozygotes (NPS/L6-NPS) and about 2% homozygotes (L6-NPS/L6-NPS) in Europeans (Table 1 and 2).

Using the publicly available data (HapMap Project and The 1,000 Genomes Project), we further examined a 500-kb genomic region that covers 888 SNPs flanking the L6-NPS SNP-*rs4751440* in 14 worldwide populations in order to investigate the origination of this SNP. Haplotype analysis suggested a single origin of the newly derived allele (Fig. 1A), with the mutation (G>C) locating in a unique, and nearly unbroken haplotype spanning ~14 kb in the CEU (Utah Residents with Northern and Western European ancestry) population (Fig. S1). Under the neutrality rule, the

Table 1. Rs4751440 (L[6]-NPS) exhibits a high frequency in Europeans based on Exome Sequencing Project.

Exome Sequencing Project	Rs4751440 allele frequency		Rs4751440 genotypes		
Population	L[6]-NPS	NPS	C/C	G/C	G/G
EuropeanAmerican	13.95%	86.05%	1.8%	24.3%	73.9%
AfricanAmerican	2.2%	97.8%	0.1%	4.19%	95.7%

The SNP rs4751440 allele frequency and genotypes were calculated based on Exome Sequencing Project.
doi:10.1371/journal.pone.0083009.t001

average age of a polymorphism with the frequency p is estimated to be $-4N_e[p(\log p)/(1-p)]$ [27,28]. With the assumption of $N_e = 5,000$ for each population, the time for the derived allele of rs4751440 to arise to its current frequency in the AFR, AMR and EUR populations is ∼11,000, ∼43,000, and ∼160,000 yrs, respectively. However, these estimations are incompatible with archaeological evidence showing that modern humans originated ∼195,000 yrs ago in Sub-Saharan Africa and migrated towards Northern Eurasia ∼40,000 yrs ago [23,24]. Alternatively, we estimated the age of rs4751440-assocatated haplotypes based on the decay of haplotypes. Assuming a recombination rate derived from estimates of linkage disequilibrium, rs4751440-assocatated haplotypes arose ∼27,000 yrs in the EUR population. We also performed another linkage disequilibrium analysis using a recombination rate ranging from 0.5–3.03 cM/Mb as used in previous studies [29–31] and an origin age of between 39,000 and 7,000 yrs was derived.

To better estimate the temporal and geographic origin for the rs4751440 allele, we performed three million forward simulations using a spatially explicit population model [20] to identify the origination and spread of allele rs4751440 in Europe. The Approximate Bayesian Computation (ABC) model [32] was used to compare simulated to observed allele frequencies and to estimate the evolutionary and demographic parameters [6]. The ABC modeling estimated that rs4751440 originated in Western Europe between 12,250 and 39,000 yrs ago (95% credible interval), with a mode of 23,650 yrs ago and a median of 25,200 yrs ago (Fig. 1B, Fig. S2, Table S2). Combined with linkage disequilibrium analysis, the rs4751440 probably originated from the ancestor of European population ∼25,000 yrs ago.

Non-synonymous mutations on mature region of peptide ligands could alter their bioactivities. The proprotein NPS is

Table 2. Rs4751440 (L[6]-NPS) exhibits a high frequency in Europeans based on Exome Sequencing Project based on Hapmap project.

HapMap Project	Rs4751440 allele frequency		Rs4751440 genotypes		
Population	L[6]-NPS	NPS	C/C	G/C	G/G
EUR	12.7%	87.3%	2.11%	21.11%	76.78%
AMR	5.5%	94.5%	0%	11.05%	88.95%
AFR	0.4%	99.6%	0%	0.81%	99.19%
ASN	0%	100%	0%	0%	100%

The SNP rs4751440 allele frequency and genotypes were calculated based on Hapmap project. Different human populations (AFR-African, AMR-Ad Mixed American, ASN-East Asian, EUR-European, SAN-South Asian) from the Hapmap project are shown.
doi:10.1371/journal.pone.0083009.t002

cleaved to the functional mature peptide with 20 residues [9] (Fig. 2A). The matured NPS shows high conservation in vertebrates and the rs4751440 SNP generates a non-synonymous substitution (V to L) on the 6th residue of NPS. This position is identical in all vertebrate species examined (Fig. 2A). The 6th valine residue is located in the hinge region of NPS, thus important in maintaining its proper conformation and mutagenesis experiments indicated this position to be essential for interactions with the NPSR receptor [33,34].

To compare the bioactivity of wide type NPS (NPS) and the SNP variant (L[6]-NPS), we monitored their receptor-activation activities in vitro using HEK293T cells over-expressing NPSR. Because NPS activates NPSR by increasing cAMP production and intracellular Ca^{2+} signaling [9,10], we used CRE- and NFAT-response elements to measure cAMP and intracellular Ca2+ signaling respectively [35,36]. As expected, treatment with wide-type NPS led to dose-dependent stimulation of both CRE- and NFAT- luciferase activities (Fig. 2B and C). We also performed the relaxin-LGR7 ligand-receptor pair [37] as a positive control for the CRE-luciferase assay. Also, gastrin-CCKB ligand-receptor pair [38] was used as a positive control for the SRE-luciferase assay. Cells transfected with the empty vector were also treated with NPS to serve as a negative control (Fig. S4).

As compared with wide-type NPS, the L[6]-NPS variant exhibited lower potencies with apparent EC_{50} values ∼16-fold for CRE-luciferase and ∼22-fold for NFAT-luciferase, respectively (CRE-luciferase activity, apparent EC_{50} values: wild type-37 nM, L[6]-NPS-586 nM; NFAT-luciferase, EC_{50}: wild type-45 nM, L[6]-NPS-975 nM) (Fig. 2 and 3). Similar signaling potencies were found when synthetic peptides were obtained from a different source (Fig. S3). Because both valine in the wild type NPS and leucine in the SNP are hydrophobic in nature, these findings suggest that the side chains of 6th residue in NPS are important for NPS signaling transduction.

To further elucidate the importance of the 6th position residue valine for NPS bioactivity, we chemically synthesized additional mutants with substitutions by other amino acids with different chemical properties (alanine-A, isoleucine-I and phenylalanine-F for hydrophobic property; asparagine-N for polar uncharged; lysine-K for positive uncharged; aspartic acid-D for negative charged). Similar to L[6]-NPS, substitution with two other hydrophobic amino acids (A and I) in NPS, showed impaired bioactivity with apparent EC_{50} values ∼5- (I[6]-NPS) and ∼15-fold (A[6]-NPS) higher than the wild type peptide in the CRE-luciferase assay (Fig. 3A). Also, all non-hydrophobic amino acid substitutions (N-, K- and D-) led to a complete loss of bioactivity (Fig. 3A). In contrast to the minimal loss of bioactivity following substitution with the hydrophobic isoleucine-I containing a small side chain, substitution with the hydrophobic phenylalanine-F containing a large side chain showed a complete loss of bioactivity, suggesting a bulky side chain on the 6th position is detrimental for NPS bioactivity. Likewise, similar changes in signaling potencies were
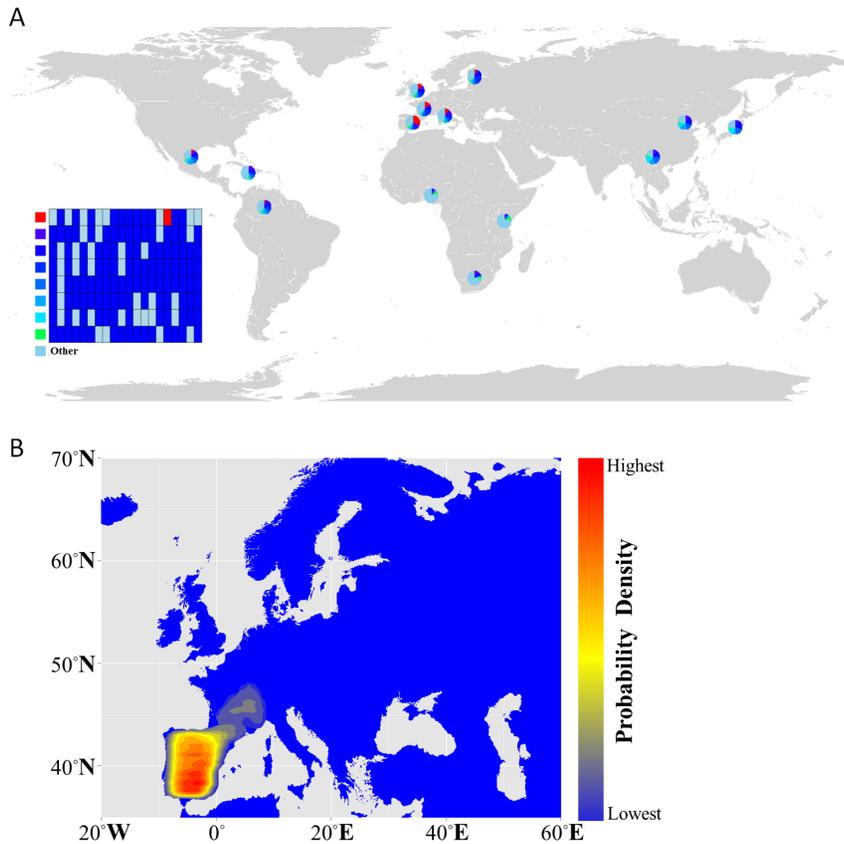
A

B

Figure 1. Origination of the L⁶-NPS variant. (**A**) Haplotype distribution of the genomic region surrounding SNP *rs4751440* based on 20 SNPs covering about 14 kb. The eight most common haplotypes are shown in the left inset, and the remaining low-frequency haplotypes are grouped as "Other." The chimpanzee allele was assumed to be the ancestral one. The *rs4751440* is shown in red whereas all other alleles are in dark blue. (**B**) The approximate posterior probability density for the geographic origin of L⁶-NPS obtained by the ABC simulation. The heat map was generated using 2D kernel density estimation of the latitude and longitude coordinates from the top ranked 5,000 of 3,000,000 simulations. Red color represents the highest probability, and blue the lowest.
doi:10.1371/journal.pone.0083009.g001

found using the NFAT-luciferase assay (Fig. 3B) when peptides with different substitutions were tested. Combining our results with earlier publications [33,34], it is clear that the 6th position valine plays a critical role in interactions with the NPSR receptor to stimulate downstream signaling pathways.

Discussion

To minimize the bias in our results, we first used all the publicly available data (the total size of ~8,000 samples) to calculate the *rs4751440* allele frequency. Secondly, we employed three different methods to investigate the origin of the *rs4751440* allele: a) the estimation of age of polymorphism under neutrality rule; b) the estimation of age of the *rs4751440*-associated haplotypes on the basis of decay of haplotypes; and c) spatially explicit population model and Approximate Bayesian Computation (ABC) inference to estimate the temporal and geographic origin of the *rs4751440* allele. The ABC method not only estimated the age of *rs4751440* allele, but also estimated the location of origin of *rs4751440* allele with addressing population stratification effect [39–41]. Also, we performed as many as 3,000,000 simulations to require the best 5,000 and 1,000 simulations to estimate the parameters of origin of *rs4751440* allele, which make the conclusion is more reliable. Based on haplotype analysis and Approximate Bayesian Computation, we concluded that the L⁶-NPS variant probably originated from the ancestor of European population ~25,000 yrs ago.

NPS, a highly conserved neuropeptide in vertebrates (Fig. 2A), plays important physiological roles in anxiety, fear, hyperactivity, food intake, and sleeping time mediated by its receptor-NPSR [9,12,15,16,18,42]. Because the SNP *rs4751440* leads to non-synonymous substitution on the 6th position (V to L) of the NPS mature region and shows ~13% of allele frequency in Europeans, heterozygous expression of L⁶-NPS is expected in 22% of Europeans whereas 2% of Europeans exclusively express L⁶-NPS (Fig. 1). Thus, 22% of Europeans with heterozygous alleles have decreased NPS bioactivity whereas the 2% of Europeans with homozygous alleles have minimal NPS activity.

Recent murine and human studies suggested the roles of NPS in diverse neural and peripheral functions, including olfaction [43], anxiolytic and anti-depressive effects [44,45], memory retention [46], monocyte chemotaxis [47], pain-related behaviors [48], neuroendocrine stress responses [49], and panicolytic-like actions [50]. Also, the NPS-NPSR system was found to be involved in addiction-related behaviors including morphine [51] and cocaine addiction [52–54]. Furthermore, the NPS-NPSR system interacts with other neural circuitry of the brain. Recent studies showed that the expression pattern of NPS and NPSR is differentially modulated by hyperthyroidism in the rat brain [55]. Also, NPS-NPSR signaling regulates the expression of several other neuropeptides, including cholecystokinin, vasoactive intestinal peptide, peptide YY, and somatostatin [56]. In addition, NPS
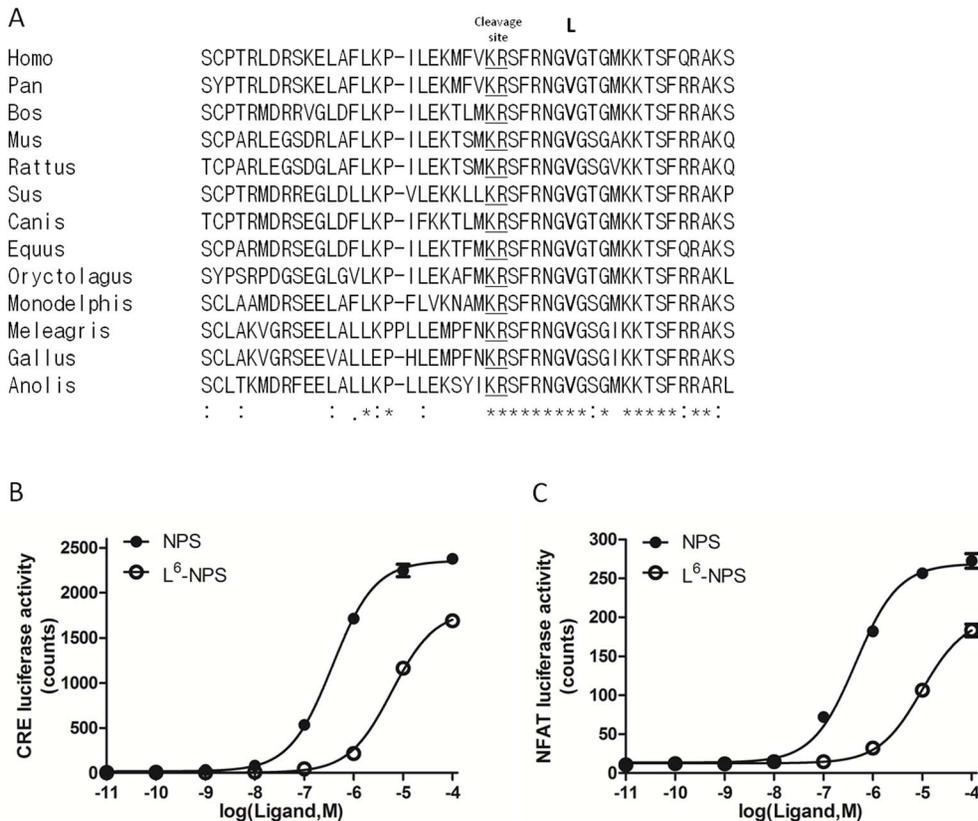
A
```
                                    Cleavage        L
                                     site
Homo          SCPTRLDRSKELAFLKP-ILEKMFVKRSFRNGVGTGMKKTSFQRAKS
Pan           SYPTRLDRSKELAFLKP-ILEKMFVKRSFRNGVGTGMKKTSFRRAKS
Bos           SCPTRMDRRVGLDFLKP-ILEKTLMKRSFRNGVGTGMKKTSFRRAKS
Mus           SCPARLEGSDRLAFLKP-ILEKTSMKRSFRNGVGSGAKKTSFRRAKQ
Rattus        TCPARLEGSDGLAFLKP-ILEKTSMKRSFRNGVGSGVKKTSFRRAKQ
Sus           SCPTRMDRREGLDLLKP-VLEKKLLKRSFRNGVGTGMKKTSFRRAKP
Canis         TCPTRMDRSEGLDFLKP-IFKKTLMKRSFRNGVGTGMKKTSFRRAKS
Equus         SCPARMDRSEGLDFLKP-ILEKTFMKRSFRNGVGTGMKKTSFQRAKS
Oryctolagus   SYPSRPDGSEGLGVLKP-ILEKAFMKRSFRNGVGTGMKKTSFRRAKL
Monodelphis   SCLAAMDRSEELAFLKP-FLVKNAMKRSFRNGVGSGMKKTSFRRAKS
Meleagris     SCLAKVGRSEELALLKPPLLEMPFNKRSFRNGVGSGIKKTSFRRAKS
Gallus        SCLAKVGRSEEVALLEP-HLEMPFNKRSFRNGVGSGIKKTSFRRAKS
Anolis        SCLTKMDRFEELALLKP-LLEKSYIKRSFRNGVGSGMKKTSFRRARL
              :   :        :  .*:*  :      ********:* *****:**:
```

Figure 2. Sequence comparison and lower NPSR receptor signaling ability of the L^6-NPS variant. (**A**) Alignment of NPS among diverse vertebrate species. Sequences were aligned by the ClustalW program [75]. Stars indicate identical amino acids and double dots (:) indicate conserved amino acids. The predicted convertase cleavage sites (KR) were underlined and the 6th amino acid "V" or "L" in the mature peptide region are shown in bold. (**B**) Comparison of NPS and L^6-NPS signaling based on the CRE-luciferase assay. (**C**) Comparison of NPS and L^6-NPS signaling based on the NFAT luciferase assay. HEK293T cells seeded in 24-well plates were co-transfected with different luciferase reporters (50 ng), the pSV-β-Gal plasmid (5 ng), and the NPSR receptor plasmid (50 ng). After 36 h, cells were cultured in serum-free media for another 18 h with increasing doses of the various NPS peptides. EC_{50} values were analyzed using Graphpad Prism 5.0.
doi:10.1371/journal.pone.0083009.g002

neurons in the locus coeruleus are activated by stress-related CRF [57]. Following intracerebroventricular injection of NPS, hypothalamic hypocretin-1/orexin-A neurons are activated [58,59]. These findings suggested that NPS-NPSR signaling affects diverse neural circuitry and brain functions.

Due to the involvement of NPS in various important brain activities, the NPSR antagonists were discovered to antagonize different physiological functions mediated by NPS [53,60–64]. The 20-aa NPS showed large conservation in vertebrate (Fig. 2). Based on structure–activity studies of NPS, the F^2, R^3, and N^4 residues constitute the message domain revealed by the chemical requirements of these positions for NPSR binding and activation. In contrast, the G^5, V^6, G^7 residues are important for shaping the bioactive conformation of the peptide [33,34]. Further study on G^5–NPS modification generated the first generation of peptidergic NPSR antagonists, including [d-Cys(tBu)^5]NPS and [d-Val^5]NPS whose antagonistic properties were confirmed *in vitro* and *in vivo* [64–67]. Also, several non-pepetidergic NPSR antagonists, including SHA 68 [63], RTI-118 [53], QA1 and PI1 [68] have been developed to block various NPS functions. However, some non-peptide antagonists showed less effect *in vivo* than *in vitro* probably due to their poor pharmacokinetic properties [68]. However, the peptidergic analogs appear to be effective both in vitro and in vivo [60,61,66]. The V^6 residue of NPS is located at

the NPS hinge region and could be essential for its bioactivity [33,34]. Our data suggest that the side chain of V6 affects the downstream signaling of NPSR (Fig. 3) and that I^6-NPS, L^6-NPS and D^6-NPS are more potent NPSR agonists. Further modifications could allow the design of agonists and antagonists as therapeutic agents.

With the completion of genome sequencing and the availability of more SNP databases, a number of NPSR gene polymorphism has also been found. Some of the SNPs in the non-coding region were found to affect the NPSR mRNA expression, whereas some SNPs in the NPSR coding region showed reduced NPSR protein membrane trafficking or reduced downstream signaling [69]. In patients, several mutations in the NPSR coding region have been associated with susceptibility to inflammatory bowel diseases [70], asthma pathogenesis [34], obsessive–compulsive disorder [71], fear-potentiated startle [72], modulates response inhibition and error monitoring [73], and macrophage immune responses [74]. It is of interest to investigate possible changes in susceptibility to these diseases in Europeans with hetero-and homozygous SNP *rs4751440* genotypes. Our study also provides the basis for future elucidation of potential phenotypic diversities between European and other populations as related to NPS signaling in the regulation of diverse brain functions.
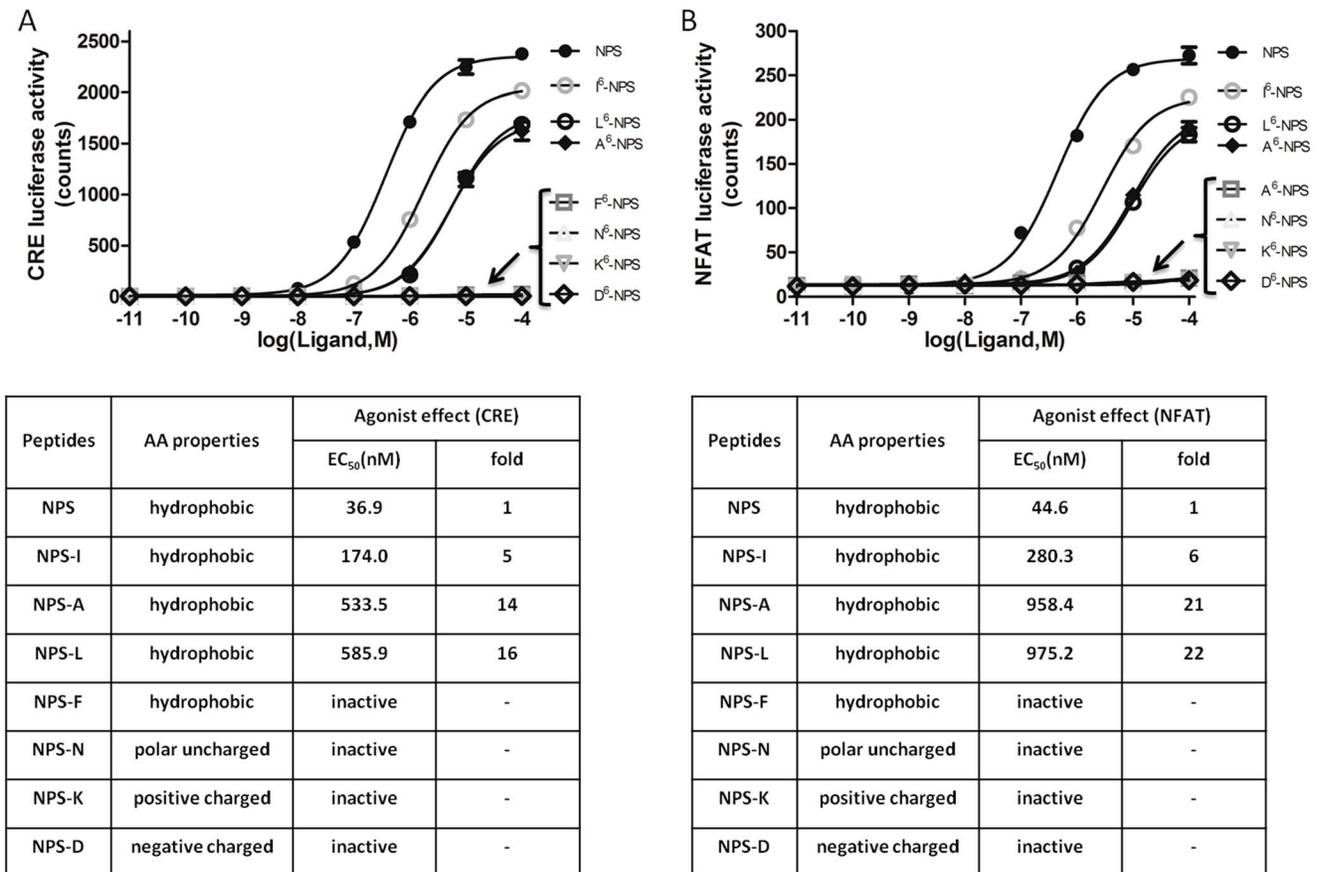
Peptides	AA properties	Agonist effect (CRE)	
		EC_{50}(nM)	fold
NPS	hydrophobic	36.9	1
NPS-I	hydrophobic	174.0	5
NPS-A	hydrophobic	533.5	14
NPS-L	hydrophobic	585.9	16
NPS-F	hydrophobic	inactive	-
NPS-N	polar uncharged	inactive	-
NPS-K	positive charged	inactive	-
NPS-D	negative charged	inactive	-

Peptides	AA properties	Agonist effect (NFAT)	
		EC_{50}(nM)	fold
NPS	hydrophobic	44.6	1
NPS-I	hydrophobic	280.3	6
NPS-A	hydrophobic	958.4	21
NPS-L	hydrophobic	975.2	22
NPS-F	hydrophobic	inactive	-
NPS-N	polar uncharged	inactive	-
NPS-K	positive charged	inactive	-
NPS-D	negative charged	inactive	-

Figure 3. Signaling abilities of different NPS mutants. (**A**) Stimulation of CRE luciferase activity mediated by NPSR in response to increasing dosages of various NPS mutants. (**B**) Stimulation of NFAT luciferase activity mediated by NPSR in response to increasing dosages of various NPS mutants. EC_{50} vales were analyzed using Graphpad Prism 5.0.
doi:10.1371/journal.pone.0083009.g003

Supporting Information

Figure S1 Linkage disequilibrium patterns of genomic regions surrounding *rs4751440*. The region surrounding SNP *rs4751440* was analyzed to include 888 SNPs over a 500 kb span in the CEU (Utah Residents with Northern and Western European ancestry) population based on the HapMap using the Haploview. An arrow denotes the location of SNP *rs4751440*. A ~14 kb block of linkage disequilibrium covering *rs4751440* is highlighted in green.
(PDF)

Figure S2 Approximate Posterior Density Estimates of Demographic and Evolutionary Parameters, Related to Figure 1B. ABC was performed retaining the top 5,000 simulations among a total of 3,000,000 simulations (tolerance level 0.17%). The posterior density estimates shown in dash blue lines are from the top 1,000 simulations (tolerance level 0.03%).
(PDF)

Figure S3 Lower NPSR receptor signaling ability of the L⁶-NPS variant. Wild type and L⁶-NPS were synthesized by the NEO Group Inc. (**A**) Comparison of NPS and L⁶-NPS signaling based on the CRE-luciferase assay. (**B**) Comparison of NPS and L6-NPS

signaling based on the NFAT-luciferase assay. Data were analyzed using Graphpad Prism 5.0.
(PDF)

Figure S4 Positive control and negative control for the CRE- and SRE- luciferase assay. No stimulation on NPS-empty vector pair for the CRE- and SRE- luciferase assay; normal stimulation on relaxin-LGR7 ligand-receptor pair for the CRE- luciferase assay and gastrin-CCKB ligand-receptor pair for the SRE-luciferase assay.
(PDF)

Table S1 SNPs causing non-synonymous substitution in the mature regions of all type A (**Table S1A**) and type B (**Table S1B**) polypeptide ligands found in the Human Plasma Membrane receptome Database.
(XLS)

Table S2 Populations used as observed data point in Figure 1.
(PDF)

Author Contributions

Conceived and designed the experiments: CD AH. Performed the experiments: CD. Analyzed the data: CD XH AH. Wrote the paper: CD XH AH.

References

1. Shastry BS (2002) SNP alleles in human disease and evolution. J Hum Genet 47: 561–566.
2. Feuk L, Carson AR, Scherer SW (2006) Structural variation in the human genome. Nat Rev Genet 7: 85–97.
3. (2003) The International HapMap Project. Nature 426: 789–796.
4. Brookes AJ (1999) The essence of SNPs. Gene 234: 177–186.
5. Chang CL, Cai JJ, Lo C, Amigo J, Park JI, et al. (2011) Adaptive selection of an incretin gene in Eurasian populations. Genome Res 21: 21–32.
6. Kamberov YG, Wang S, Tan J, Gerbault P, Wark A, et al. (2013) Modeling recent human evolution in mice by expression of a selected EDAR variant. Cell 152: 691–702.
7. Lappalainen J, Kranzler HR, Malison R, Price LH, Van Dyck C, et al. (2002) A functional neuropeptide Y Leu7Pro polymorphism associated with alcohol dependence in a large population sample from the United States. Arch Gen Psychiatry 59: 825–831.
8. Faure S, Meyer L, Costagliola D, Vaneensberghe C, Genin E, et al. (2000) Rapid progression to AIDS in HIV+ individuals with a structural variant of the chemokine receptor CX3CR1. Science 287: 2274–2277.
9. Xu YL, Reinscheid RK, Huitron-Resendiz S, Clark SD, Wang Z, et al. (2004) Neuropeptide S: a neuropeptide promoting arousal and anxiolytic-like effects. Neuron 43: 487–497.
10. Reinscheid RK, Xu YL, Okamura N, Zeng J, Chung S, et al. (2005) Pharmacological characterization of human and murine neuropeptide s receptor variants. J Pharmacol Exp Ther 315: 1338–1345.
11. Xu YL, Gall CM, Jackson VR, Civelli O, Reinscheid RK (2007) Distribution of neuropeptide S receptor mRNA and neurochemical characteristics of neuropeptide S-expressing neurons in the rat brain. J Comp Neurol 500: 84–102.
12. Jungling K, Seidenbecher T, Sosulina L, Lesting J, Sangha S, et al. (2008) Neuropeptide S-mediated control of fear expression and extinction: role of intercalated GABAergic neurons in the amygdala. Neuron 59: 298–310.
13. Meis S, Bergado-Acosta JR, Yanagawa Y, Obata K, Stork O, et al. (2008) Identification of a neuropeptide S responsive circuitry shaping amygdala activity via the endopiriform nucleus. PLoS One 3: e2695.
14. Liu X, Zeng J, Zhou A, Theodorsson E, Fahrenkrug J, et al. (2011) Molecular fingerprint of neuropeptide S-producing neurons in the mouse brain. J Comp Neurol 519: 1847–1866.
15. Okamura N, Reinscheid RK (2007) Neuropeptide S: a novel modulator of stress and arousal. Stress 10: 221–226.
16. Leonard SK, Dwyer JM, Sukoff Rizzo SJ, Platt B, Logue SF, et al. (2008) Pharmacology of neuropeptide S in mice: therapeutic relevance to anxiety disorders. Psychopharmacology (Berl) 197: 601–611.
17. Rizzi A, Vergura R, Marzola G, Ruzza C, Guerrini R, et al. (2008) Neuropeptide S is a stimulatory anxiolytic agent: a behavioural study in mice. Br J Pharmacol 154: 471–479.
18. Smith KL, Patterson M, Dhillo WS, Patel SR, Semjonous NM, et al. (2006) Neuropeptide S stimulates the hypothalamo-pituitary-adrenal axis and inhibits food intake. Endocrinology 147: 3510–3518.
19. Scheet P, Stephens M (2006) A fast and flexible statistical model for large-scale population genotype data: applications to inferring missing genotypes and haplotypic phase. American journal of human genetics 78: 629–644.
20. Itan Y, Powell A, Beaumont MA, Burger J, Thomas MG (2009) The origins of lactase persistence in Europe. PLoS computational biology 5: e1000491.
21. Bertorelle G, Benazzo A, Mona S (2010) ABC as a flexible framework to estimate demography over space and time: some cons, many pros. Molecular ecology 19: 2609–2625.
22. Itan Y, Powell A, Beaumont MA, Burger J, Thomas MG (2009) The origins of lactase persistence in Europe. PLoS Comput Biol 5: e1000491.
23. Klein RG (2009) Darwin and the recent African origin of modern humans. Proceedings of the National Academy of Sciences of the United States of America 106: 16007–16009.
24. McDougall I, Brown FH, Fleagle JG (2005) Stratigraphic placement and age of modern humans from Kibish, Ethiopia. Nature 433: 733–736.
25. Ben-Shlomo I, Yu Hsu S, Rauch R, Kowalski HW, Hsueh AJ (2003) Signaling receptome: a genomic and evolutionary perspective of plasma membrane receptors involved in signal transduction. Sci STKE 2003: RE9.
26. Ben-Shlomo I, Rauch R, Avsian-Kretchmer O, Hsueh AJ (2007) Matching receptome genes with their ligands for surveying paracrine/autocrine signaling systems. Mol Endocrinol 21: 2009–2014.
27. Kimura M, Ota T (1973) The age of a neutral mutant persisting in a finite population. Genetics 75: 199–212.
28. Slatkin M, Rannala B (2000) Estimating allele age. Annual review of genomics and human genetics 1: 225–249.
29. Broman KW, Murray JC, Sheffield VC, White RL, Weber JL (1998) Comprehensive human genetic maps: individual and sex-specific variation in recombination. American journal of human genetics 63: 861–869.
30. Dib C, Faure S, Fizames C, Samson D, Drouot N, et al. (1996) A comprehensive genetic map of the human genome based on 5,264 microsatellites. Nature 380: 152–154.
31. Kong A, Gudbjartsson DF, Sainz J, Jonsdottir GM, Gudjonsson SA, et al. (2002) A high-resolution recombination map of the human genome. Nature genetics 31: 241–247.
32. Beaumont MA, Zhang W, Balding DJ (2002) Approximate Bayesian computation in population genetics. Genetics 162: 2025–2035.
33. Roth AL, Marzola E, Rizzi A, Arduin M, Trapella C, et al. (2006) Structure-activity studies on neuropeptide S: identification of the amino acid residues crucial for receptor activation. J Biol Chem 281: 20809–20816.
34. Bernier V, Stocco R, Bogusky MJ, Joyce JG, Parachoniak C, et al. (2006) Structure-function relationships in the neuropeptide S receptor: molecular consequences of the asthma-associated mutation N107I. J Biol Chem 281: 24704–24712.
35. Cheng Z, Garvin D, Paguio A, Stecha P, Wood K, et al. (2010) Luciferase Reporter Assay System for Deciphering GPCR Pathways. Curr Chem Genomics 4: 84–91.
36. Wang CJ, Hsu SH, Hung WT, Luo CW (2009) Establishment of a chimeric reporting system for the universal detection and high-throughput screening of G protein-coupled receptors. Biosens Bioelectron 24: 2298–2304.
37. Hsu SY, Nakabayashi K, Nishi S, Kumagai J, Kudo M, et al. (2002) Activation of orphan receptors by the hormone relaxin. Science 295: 671–674.
38. Todisco A, Takeuchi Y, Urumov A, Yamada J, Stepan VM, et al. (1997) Molecular mechanisms for the growth factor action of gastrin. Am J Physiol 273: G891–898.
39. Devlin B, Roeder K (1999) Genomic control for association studies. Biometrics 55: 997–1004.
40. Bacanu SA, Devlin B, Roeder K (2002) Association studies for quantitative traits in structured populations. Genet Epidemiol 22: 78–93.
41. Price AL, Patterson NJ, Plenge RM, Weinblatt ME, Shadick NA, et al. (2006) Principal components analysis corrects for stratification in genome-wide association studies. Nat Genet 38: 904–909.
42. Rizzi A, Vergura R, Marzola G, Ruzza C, Guerrini R, et al. (2008) Neuropeptide S is a stimulatory anxiolytic agent: a behavioural study in mice. British Journal of Pharmacology 154: 471–479.
43. Shao YF, Zhao P, Dong CY, Li J, Kong XP, et al. (2013) Neuropeptide S facilitates mice olfactory function through activation of cognate receptor-expressing neurons in the olfactory cortex. PLoS One 8: e62089.
44. Dine J, Ionescu IA, Stepan J, Yen YC, Holsboer F, et al. (2013) Identification of a role for the ventral hippocampus in neuropeptide S-elicited anxiolysis. PLoS One 8: e60219.
45. Enquist J, Ferwerda M, Madhavan A, Hok D, Whistler JL (2012) Chronic ethanol potentiates the effect of neuropeptide s in the basolateral amygdala and shows increased anxiolytic and anti-depressive effects. Neuropsychopharmacology 37: 2436–2445.
46. Han RW, Zhang RS, Xu HJ, Chang M, Peng YL, et al. (2013) Neuropeptide S enhances memory and mitigates memory impairment induced by MK801, scopolamine or Abeta(1)(-)(4)(2) in mice novel object and object location recognition tasks. Neuropharmacology 70: 261–267.
47. Filaferro M, Novi C, Ruggieri V, Genedani S, Alboni S, et al. (2013) Neuropeptide S stimulates human monocyte chemotaxis via NPS receptor activation. Peptides 39: 16–20.
48. Ren W, Kiritoshi T, Gregoire S, Ji G, Guerrini R, et al. (2013) Neuropeptide S: a novel regulator of pain-related amygdala plasticity and behaviors. J Neurophysiol.
49. Kumsta R, Chen FS, Pape HC, Heinrichs M (2013) Neuropeptide S receptor gene is associated with cortisol responses to social stress in humans. Biol Psychol 93: 304–307.
50. Pulga A, Ruzza C, Rizzi A, Guerrini R, Calo G (2012) Anxiolytic- and panicolytic-like effects of Neuropeptide S in the mouse elevated T-maze. Eur J Neurosci 36: 3531–3537.
51. Ghazal P, Ciccocioppo R, Ubaldi M (2013) Morphine dependence is associated with changes in neuropeptide S receptor expression and function in rat brain. Peptides 46: 6–12.
52. Kallupi M, de Guglielmo G, Cannella N, Li HW, Calo G, et al. (2013) Hypothalamic neuropeptide S receptor blockade decreases discriminative cue-induced reinstatement of cocaine seeking in the rat. Psychopharmacology (Berl) 226: 347–355.
53. Schmoutz CD, Zhang Y, Runyon SP, Goeders NE (2012) Antagonism of the neuropeptide S receptor with RTI-118 decreases cocaine self-administration and cocaine-seeking behavior in rats. Pharmacol Biochem Behav 103: 332–337.
54. Cannella N, Kallupi M, Ruggeri B, Ciccocioppo R, Ubaldi M (2013) The role of the neuropeptide S system in addiction: focus on its interaction with the CRF and hypocretin/orexin neurotransmission. Prog Neurobiol 100: 48–59.
55. Gonzalez CR, Martinez de Morentin PB, Martinez-Sanchez N, Gomez-Diaz C, Lage R, et al. (2012) Hyperthyroidism differentially regulates neuropeptide S system in the rat brain. Brain Res 1450: 40–48.
56. Camilleri M, Carlson P, Zinsmeister AR, McKinzie S, Busciglio I, et al. (2010) Neuropeptide S receptor induces neuropeptide expression and associates with intermediate phenotypes of functional gastrointestinal disorders. Gastroenterology 138: 98–107 e104.
57. Jungling K, Liu X, Lesting J, Coulon P, Sosulina L, et al. (2012) Activation of neuropeptide S-expressing neurons in the locus coeruleus by corticotropin-releasing factor. J Physiol 590: 3701–3717.

58. Niimi M (2006) Centrally administered neuropeptide S activates orexin-containing neurons in the hypothalamus and stimulates feeding in rats. Endocrine 30: 75–79.

59. Zhao P, Shao YF, Zhang M, Fan K, Kong XP, et al. (2012) Neuropeptide S promotes wakefulness through activation of the posterior hypothalamic histaminergic and orexinergic neurons. Neuroscience 207: 218–226.

60. Ruzza C, Rizzi A, Camarda V, Pulga A, Marzola G, et al. (2012) [tBu-D-Gly5]NPS, a pure and potent antagonist of the neuropeptide S receptor: in vitro and in vivo studies. Peptides 34: 404–411.

61. Cifani C, Micioni Di Bonaventura MV, Cannella N, Fedeli A, Guerrini R, et al. (2011) Effect of neuropeptide S receptor antagonists and partial agonists on palatable food consumption in the rat. Peptides 32: 44–50.

62. Thorsell A, Tapocik JD, Liu K, Zook M, Bell L, et al. (2013) A novel brain penetrant NPS receptor antagonist, NCGC00185684, blocks alcohol-induced ERK-phosphorylation in the central amygdala and decreases operant alcohol self-administration in rats. J Neurosci 33: 10132–10142.

63. Okamura N, Habay SA, Zeng J, Chamberlin AR, Reinscheid RK (2008) Synthesis and pharmacological in vitro and in vivo profile of 3-oxo-1,1-diphenyl-tetrahydro-oxazolo[3,4-a]pyrazine-7-carboxylic acid 4-fluoro-benzylamide (SHA 68), a selective antagonist of the neuropeptide S receptor. J Pharmacol Exp Ther 325: 893–901.

64. Camarda V, Rizzi A, Ruzza C, Zucchini S, Marzola G, et al. (2009) In vitro and in vivo pharmacological characterization of the neuropeptide s receptor antagonist [D-Cys(tBu)5]neuropeptide S. J Pharmacol Exp Ther 328: 549–555.

65. Guerrini R, Salvadori S, Rizzi A, Regoli D, Calo G (2010) Neurobiology, pharmacology, and medicinal chemistry of neuropeptide S and its receptor. Med Res Rev 30: 751–777.

66. Guerrini R, Camarda V, Trapella C, Calo G, Rizzi A, et al. (2009) Synthesis and biological activity of human neuropeptide S analogues modified in position 5: identification of potent and pure neuropeptide S receptor antagonists. J Med Chem 52: 524–529.

67. Peng YL, Han RW, Chang M, Zhang L, Zhang RS, et al. (2010) Central Neuropeptide S inhibits food intake in mice through activation of Neuropeptide S receptor. Peptides 31: 2259–2263.

68. Camarda V, Ruzza C, Rizzi A, Trapella C, Guerrini R, et al. (2013) In vitro and in vivo pharmacological characterization of the novel neuropeptide S receptor ligands QA1 and PI1. Peptides 48C: 27–35.

69. Anedda F, Zucchelli M, Schepis D, Hellquist A, Corrado L, et al. (2011) Multiple polymorphisms affect expression and function of the neuropeptide S receptor (NPSR1). PLoS One 6: e29523.

70. D'Amato M, Bruce S, Bresso F, Zucchelli M, Ezer S, et al. (2007) Neuropeptide s receptor 1 gene polymorphism is associated with susceptibility to inflammatory bowel disease. Gastroenterology 133: 808–817.

71. Lennertz L, Franke PE, Grabe HJ, Rampacher F, Schulze-Rauschenbach S, et al. (2013) The functional coding variant Asn107Ile of the neuropeptide S receptor gene (NPSR1) influences age at onset of obsessive-compulsive disorder. Int J Neuropsychopharmacol 16: 1951–1958.

72. Glotzbach-Schoon E, Andreatta M, Reif A, Ewald H, Troger C, et al. (2013) Contextual fear conditioning in virtual reality is affected by 5HTTLPR and NPSR1 polymorphisms: effects on fear-potentiated startle. Front Behav Neurosci 7: 31.

73. Beste C, Konrad C, Uhlmann C, Arolt V, Zwanzger P, et al. (2013) Neuropeptide S receptor (NPSR1) gene variation modulates response inhibition and error monitoring. Neuroimage 71: 1–9.

74. Pulkkinen V, Majuri ML, Wang G, Holopainen P, Obase Y, et al. (2006) Neuropeptide S and G protein-coupled receptor 154 modulate macrophage immune responses. Hum Mol Genet 15: 1667–1679.

75. Thompson JD, Higgins DG, Gibson TJ (1994) CLUSTAL W: improving the sensitivity of progressive multiple sequence alignment through sequence weighting, position-specific gap penalties and weight matrix choice. Nucleic Acids Res 22: 4673–4680.